Journal of Hydrology 484 (2013) 55–62

Contents lists available at SciVerse ScienceDirect

Journal of Hydrology

journal homepage: www.elsevier.com/locate/jhydrol

Multimethod assessment of evapotranspiration shifts due to non-irrigated agricultural development in Sweden

Fernando Jaramillo *, Carmen Prieto, Steve W. Lyon, Georgia Destouni

Department of Physical Geography and Quaternary Geology, Bert Bolin Centre for Climate Research, Stockholm University, SE-106 91 Stockholm, Sweden

ARTICLE INFO

Article history:
Received 20 October 2012
Accepted 12 January 2013
Available online 24 January 2013
This manuscript was handled by Konstantine P. Georgakakos, Editor-in-Chief, with the assistance of Matthew Rodell, Associate Editor

Keywords:
Evapotranspiration
Climate change
Land use change
Agriculture
Hydrological flow partitioning
Hydroclimatic change

SUMMARY

During the 20th century, Sweden underwent a persistent agricultural development. In this study, we use and combine historical hydroclimatic and agricultural data to investigate how this large scale change of land use, and subsequent intensification of crop production, affected regional hydrology in two adjacent Swedish drainage basins. We find a main increase of evapotranspiration (ET) as cultivated area and/or crop production increased during the period 1901–1940. Thereafter, ET stabilized at a new higher level. Comparison between the data given, water balance constrained ET quantification (ET_{wb}), and a range of different comparative estimates of purely climate driven ET (ET_{clim}) shows that only 31% of the steep 1901–1940 increase of ET_{wb} can be explained by climate change alone. The remaining 69% of this ET_{wb} shift, which occurred in both investigated drainage basins, is instead explainable to large degree by the regional land use conversion from seminatural grasslands to cultivated land and associated enhanced productivity of herbaceous species.

1. Introduction

Vegetation interacts dynamically with climate at different scales to regulate water balance and the partitioning of precipitation into evapotranspiration and runoff (Asokan et al., 2010; Destouni et al., 2013; Donohue et al., 2007; Douglas et al., 2006; Gordon et al., 2005; Shibuo et al., 2007). Agricultural development (increase in area and/or production) involves changes of vegetation and consequent biogeophysical land properties such as surface albedo, roughness length, rooting depth and leaf/stem area index, which can all affect the evapotranspiration rate at a given land surface (Kvalevag et al., 2010). Agricultural effects on hydrological flow partitioning depend on factors such as the original, predevelopment coverage of vegetation, the introduced type of agricultural crops, and additionally on whether irrigation is used in the agricultural development.

Land use changes such as deforestation may decrease evapotranspiration and increase runoff, while establishment of forest on sparsely vegetated land may have an opposite effect (Gordon et al., 2005; Vanlill et al., 1980). Conversion of unplowed land in natural and/or seminatural conditions into agricultural crops may increase evapotranspiration (Destouni et al., 2013; Loarie et al., 2011), but under some conditions may decrease it (Schilling et al., 2008), while a change from agriculture to forests by cultivation abandonment may initially decrease evapotranspiration (Qiu et al., 2011) and later increase it (Donohue et al., 2007). In general, the dynamics of agricultural development and its impacts on the hydrological cycle need to be understood under a variety of land use, climate and hydrological catchment conditions (Destouni et al., 2013).

It is then difficult to separate the impact of land use changes from those of climatic change on hydrological flow partitioning, since many climatic and biogeophysical parameters combine to affect the rates of evapotranspiration. The capability of distinguishing the effects of different drivers depends on available data and the development of different methods to interpret them for such distinction (e.g., Destouni et al., 2010a, 2013; Shibuo et al., 2007; Tomer and Schilling, 2009; Wang and Hejazi, 2011). Methodological development is important for understanding the different change drivers and their impacts in the past, as well as for accurately projecting impacts in the future and applying appropriate management measures for society's adaptation to them (Jarsjö et al., 2012). Recent technology such as MODIS (King et al., 1992) and other satellite imagery products (Zhang et al., 2010) have provided new tools for such separation, but only for studying relatively recent time periods that overlap with the accessibility to these technologies (e.g., Cheng et al., 2011; Douglas et al., 2006;

* Corresponding author. Tel.: +46 8 16 4665.
E-mail addresses: fernando.jaramillo@natgeo.su.se (F. Jaramillo), carmen.prieto@natgeo.su.se (C. Prieto), steve.lyon@natgeo.su.se (S.W. Lyon), georgia.destouni@natgeo.su.se (G. Destouni).

0022-1694
http://dx.doi.org/10.1016/j.jhydrol.2013.01.010

Loarie et al., 2011). For earlier times, the study of historical land use and associated evapotranspiration changes can for instance be approached by a catchment wise water balance assessment depending on the availability of hydroclimatic and land use data (Asokan et al., 2010; Destouni et al., 2010a, 2013; Shibuo et al., 2007). Furthermore, remote sensing and basin wise assessment of water balance changes can also be fruitfully combined to distinguish water storage changes as additional components of total hydrological change (Karlsson et al., 2012).

In previous studies of hydroclimatic change due to agricultural developments, great emphasis has been put on irrigation, which has been shown to impact climate change in addition to water resources (Bonfils and Lobell, 2007; Boucher et al., 2004; Destouni et al., 2010a; Kueppers et al., 2007; Lobell et al., 2009). However, also non-irrigated agriculture has recently been shown to have similar change impacts on evapotranspiration and thus hydrological flow partitioning, with important global implications (Destouni et al., 2013), not least in view of rising food demands due to the world's growing population (Gordon et al., 2003). Testing and quantifying possible impacts of non-irrigated agriculture, which is much more common worldwide than irrigated agriculture, should then be a priority for hydrological research across a variety of different regions.

In the present study, we investigate effects of non-irrigated agriculture on evapotranspiration and hydrological flow partitioning in two Swedish agricultural drainage basins. For both of these basins, availability of historical hydroclimatic data on temperature, precipitation, wind, lake levels and runoff extends back to the beginning of the 20th century, as does also available information on agriculture (cultivated area and crop yields), which is needed to distinguish the possible agricultural effects on historic hydroclimatic change. As the study seeks to understand these effects on regional water balance and hydrological flow partitioning, it uses a multimethod approach to particularly test and separate the effects of land use change from those of climate change on long term evapotranspiration changes.

2. Study site description

This study uses the hydrologicaly well investigated Swedish Norrström Drainage Basin (NDB) (see, e.g., Destouni and Darracq (2009), Destouni et al. (2010b) and further references therein) as its main case, along with the neighboring Motala Ström Drainage Basin (MSDB) for interbasin comparison (Fig. 1a). Approximately 20% of the Swedish population lives within the NDB area (22 650 km^2) mainly concentrated in the cities of Stockholm, Uppsala, Västeras and Örebro (less than 4% of its area). The basin is also recognized as a hot spot for nutrient loading into the Baltic Sea, due to both its agricultural activity and the size of its population.

About 1300 lakes are spread within the NDB and account for 11% of its total area. Water draining from the NDB flows into the Baltic Sea through four outlets of Lake Mälaren (third largest lake in Sweden, 1078 km^2), three of which are located in the city of Stockholm. Lake Mälaren started to be regulated in 1943 to stop salt water intrusion from the Baltic Sea and to avoid flooding of the Stockholm metropolitan area (Granström, 2003). Its regulation is thus not intended for electricity production or water storage. The other major lake in the NDB, Lake Hjälmaren (fourth largest in Sweden, 477 km^2), drains its waters into Lake Mälaren. Lake Hjälmaren started to be regulated between 1878 and 1888 in order to drain approximately 160 km^2 of land for agricultural use (Norell, 2001).

The elevation of the NDB varies between sea level and 460 m.a.s.l. from south-east to north-west, with land use also changing along this direction. The hills in the north-west of the basin are covered by temperate forest while the center of the basin and the major lake area in the south and east are characterized by open areas comprised mainly of grasslands and agricultural systems. Forests and open areas currently occupy 48% and 36% of the NDB area, respectively. The mean annual precipitation over the 20th century averaged 590 mm/yr as calculated from data by Mitchell and Jones (2005), which is more than double the corresponding mean annual runoff, 227 mm/yr, as calculated from data by the Swedish Meteorological and Hydrological Institute (SMHI, 2010). The basin typically experiences seasonal snowfall during winter that melts and joins the surface runoff during spring.

The neighboring MSDB has similar characteristics as the NDB; it includes a large water body (here the second largest lake in Sweden, Lake Vättern, 3540 km^2) and has similar types of soil, vegetation and historical agricultural development. The 13,283 km^2 of the basin are currently composed of forests (51%) and open land (24%). Most of the agricultural area is in the plains located between Lake Vättern, the Motala Ström River, and the Roxen and Sommen lakes. About 890 surface water bodies in the MSDB account for 22% of its area. Major urban centers include Linköping, Jönköping at the south of Lake Vättern, and Nyköping at the outlet of the Motala Ström River into the Baltic Sea.

The expansion of agriculture in the NDB and MSDB region began in the second half of the 19th century with gradual conversion of original seminatural grasslands to agricultural land (Jansson et al., 2011) (Fig. 1b). The seminatural grasslands located on fertile peat and clay soils were further gradually drained by ditches to expand the plowed land devoted to ley for fodder and cereals (Dahlström et al., 2006). These developments continued until the 1920s when the historical peak of agricultural area was reached. At this time, approximately 20% and 16% of the area of the NDB and MSDB, respectively, was used for agricultural cultivation. From this point to the present, cultivated area has been steadily decreasing accompanied by an increase in forest coverage that, in most cases, arises by natural succession. Even though cultivated area decreased, the crop yields from it continued to increase, mainly due to the introduction of fertilizers and to the abandonment of cereal and ley production rotation (Saifi and Drake, 2008). Currently, crop production in the NDB and MSDB is comprised of cereals (36%), ley (33%), and other crops (31%) such as potatoes, linseed, fodder roots and various types of beans.

3. Materials and methods

In order to distinguish effects of climate and land use changes on hydrological flow partitioning, and more specifically on actual evapotranspiration (AET), we estimated AET by different methods, including a basic, water balance constrained calculation of AET (denoted AET_{wb}) based on the water budget in each basin as given and constrained by the basin data. The AET_{wb} measure includes effects of both climatic and land use change, and its calculation is described further in Section 3.1. Furthermore, we calculated different comparative AET measures with a multimethod assessment approach that uses different combinations of theoretical and empirical climate driven AET models (with results denoted AET_{clim}), in order to distinguish the AET changes driven by climate change alone. Since this comparative multimethod assessment approach (described further in Section 3.2) aimed at distinguishing the effects of only climatic change, all parameters related to land use, such as albedo or plant water availability, were left unchanged through time in all AET_{clim} calculations.

Moreover, by directly comparing change slopes (denoted $sAET_{wb}$ and $sAET_{clim}$) obtained for 20-year moving averages (to filter the large noise of interannual variability) of the different AET

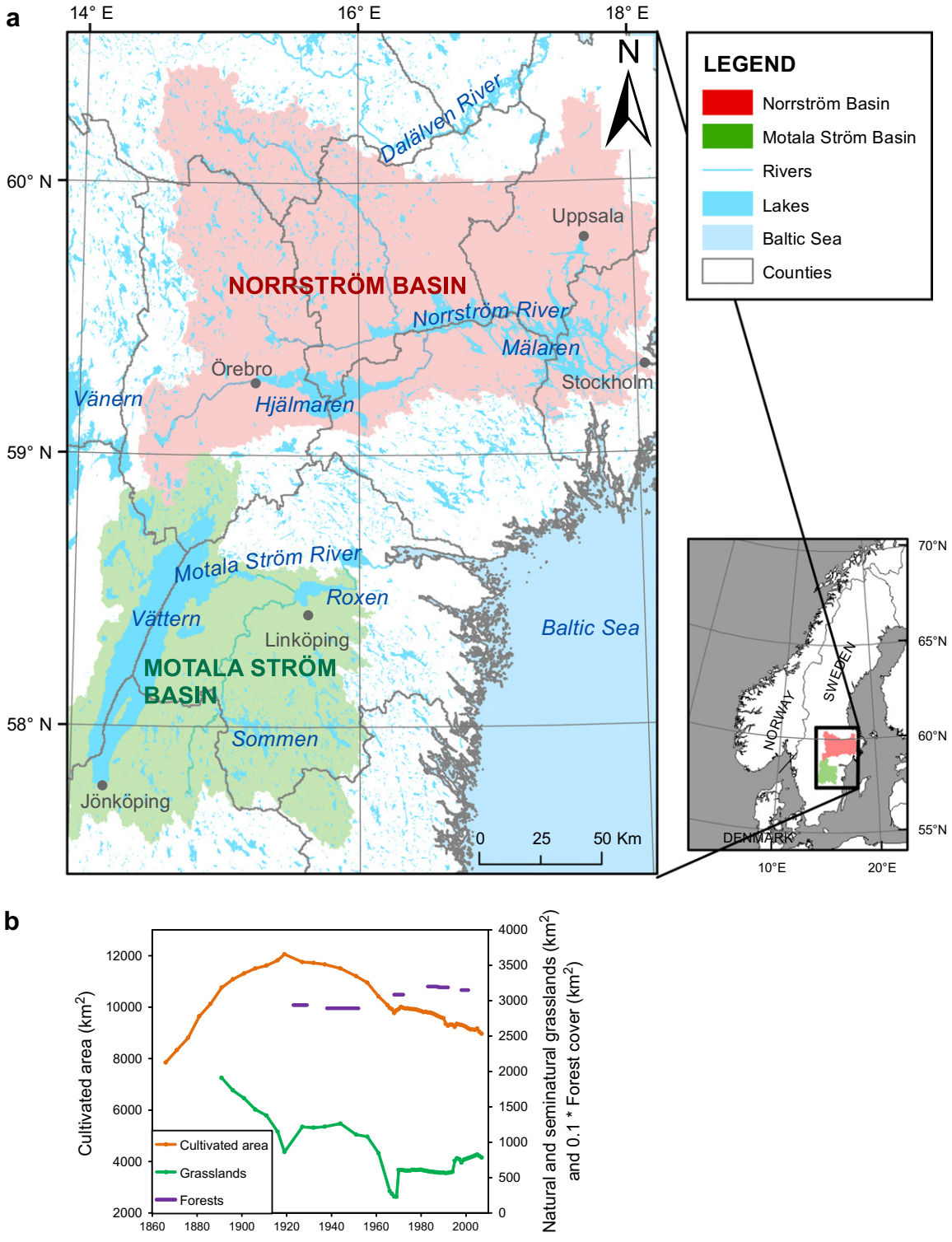

Fig. 1. Locations of the study basins and their related land use changes. (a) The study basins, Norrström Drainage Basin (NDB) and Motala Ström Drainage Basin (MSDB), and their main water bodies. (b) Land use development and changes in the two basins, from the end of the 19th century to the end of the 20th century.

measures over the 20th century (AET_{wb} and AET_{clim}, respectively), we could determine if climate change alone (i.e., if any of the possible AET_{clim} measures) could sufficiently explain the changes in AET_{wb} given by the historically recorded data. The slope comparison approach is described in Section 3.3, and the hydroclimatic and agricultural development data underlying the AET change quantifications and interpretations are described in Sections 3.4 and 3.5.

3.1. Water balance constrained assessment of AET_{wb}

We used the basic water balance equation:

$$AET_{wb} = P - Q - \Delta S \quad (1)$$

to estimate AET_{wb}, where P is annual precipitation, Q is annual runoff and ΔS is annual change in water storage in each drainage basin. Availability of water level, L, data over the whole 20th

century for Lake Mälaren in the NDB and Lake Vättern in the MSDB enabled estimates of AET_{wb} for a range of different possible ΔS assumptions. Specifically, we considered three different possible ΔS scenarios when determining AET_{wb} from Eq. (1): (1) Assuming that there is no annual water storage change in the drainage basin, such that $\Delta S = 0$ (yielding estimate AET_{wb1}), (2) Assuming that water storage change occurs only in the main large lake, for which L data is available, such that ΔS equals the data given change in lake volume divided by the total area of the drainage basin (yielding AET_{wb2}), (3) Assuming the same surface water and groundwater level changes over the whole drainage basin as in the main large lake, for which L data is available, such that ΔS equals the data given change in L (yielding AET_{wb3}).

3.2. Multimethod assessment of climate driven AET_{clim}

For comparison with AET_{wb}, we calculated AET_{clim} by four different combinations (Table 1) of Potential Evapotranspiration E_o and AET models ($AET_{clim1-4}$). Combinations 1 and 2 involve the E_o model by Langbein (1949) and the AET models by Turc (1954) and Budyko (1974), which constitute relatively simple ways to calculate AET_{clim} since they are only expressed in terms of mean annual temperature T and precipitation P. Combinations 3 and 4 are not purely climate driven, since both Priestley and Taylor (1971) and FAO Penmann–Monteith by Allen (1998) (for E_o calculation, Table 1) consider the influence of vegetation on E_o through the dependence of surface albedo on net radiation (R_n). Similarly, Zhang et al. (2001) (for AET_{clim} calculation based on E_o, Table 1) uses a plant available water coefficient w to account for vegetation effects on AET. Combinations 3 and 4 were then here used for assessment of climate driven AET_{clim}, by keeping the albedo and w measures constant in time.

3.3. Comparison of long term slope change of AET_{wb} and AET_{clim}

For time periods with greater absolute values of $sAET_{wb}$ than corresponding values of $sAET_{clim}$, one may infer that the data given AET_{wb} change trend quantified by $sAET_{wb}$ is not fully explained by the (also data given) climatic change in those periods. This implies that $sAET_{wb}$ may then be influenced by land use change, predominantly if $sAET_{wb}$ is much greater than $sAET_{clim}$, or at least additional to (and in the same direction as) the climatic change influence. In contrast, when the absolute value of $sAET_{wb}$ is about equal or smaller than that of $sAET_{clim}$, the data given change trend in AET_{wb} may: (1) be fully explained by the climate change alone; or (2) be determined by opposing, and thus in combination dampening effects on AET_{wb} of the climate and land use changes. Analysis of Covariance (ANCOVA) was used to compare the slopes of linear regressions to the changing 20-year averages of AET_{wb} and the AET_{clim} combination calculations. Signals of land use change could then be distinguished from those of climate change when the $sAET_{wb}$ value differed significantly from all different $sAET_{clim}$ possible calculations (combinations in Table 1), at the $\alpha = 0.01$ significance level.

3.4. Hydroclimatic data

For the AET_{wb} calculations, R data for both NDB and MSDB, and L data for Mälaren and Vättern Lakes were obtained from SMHI (2010). The shape and area of each drainage basin were also obtained from the same reference. The monthly total precipitation and monthly mean temperature were downloaded for each CRU cell within the drainage basins from the Climatic Research Unit Database (CRU TS 2.1) of the Consortium of Spatial Information of the Consultative Group on International Agricultural Research (CGIAR-CSI) (Mitchell and Jones, 2005). This dataset has a monthly $0.5^\circ \times 0.5^\circ$ grid over the period 1901–2002. We aggregated the monthly values to annual values and then calculated a CRU cell area weighted average, which was also used in the calculation of annual E_o underlying AET_{clim} combinations 1 and 2, as well as for the AET_{clim} calculations in all combinations (Table 1).

Linear regression between P calculated from CRU and P calculated by Thiessen Polygons using the complete set of all operational SMHI station data within and in the vicinity of NDB (a maximum of 36 available stations for the period 1970–1993 and a minimum of seven stations for the period 1901–1908) yielded $R^2 = 0.84$, showing the capability of the CRU P data to represent the P climatology of the NDB. Furthermore, the standard deviation of annual P between 1901 and 2002 was calculated for the NDB to be 86 mm/yr based on CRU data and 92 mm/yr based on SMHI data. Similar standard deviation of 82 mm/yr was also calculated for P in MSDB, and is generally characteristic of interannual P variability in the region of South and Central Sweden. The number of stations used for a given annual P from CRU varies in time. Between 1901 and 1990, Mitchell and Jones (2005) calculate P from an average of 69 stations for the NDB, with 49 stations being the smallest number used for P calculation in a CRU cell; corresponding average and minimum number of stations for the MSDB were 66 and 53, respectively. However, for the period 1990–2002 these values drop to an average of 16 stations for both basins and a minimum of 7 and 8 stations for each P CRU cell, for NDB and MSDB, respectively.

For daily E_o estimates in AET_{clim} combinations 3 and 4 (Table 1), the maximum and minimum monthly temperatures (T_{max} and T_{min}) per CRU cell were also obtained from Mitchell and Jones (2005) and assumed to apply for all days of that given month. Net radiation R_n for both FAO Penman–Monteith and Priestley and Taylor (1971) was calculated according to the methodology suggested by Allen (1998). Solar radiation R_s was estimated with Eq. (50) of Allen (1998), which is also expressed in terms of T_{min} and T_{max}. A constant mean albedo of 0.23 was used for all surfaces in the E_o calculations (see further Table 1 for other constant values). Atmospheric pressure was used for the calculation of both the psychometric constant (γ) and R_n. Actual vapor pressure e_a

Table 1
Multimethod combinations of Potential evapotranspiration (E_o) and actual evapotranspiration (AET_{clim}) functions of E_o.

	Potential evapotranspiration E_o		Actual evapotranspiration AET	
Combination 1	Langbein (1949)	$E_o = -325 + 21T + 0.9T^2$	Turc (1954)	$AET_{clim1} = P[0.9 + (\frac{P}{E_o})^2]^{0.5}$
Combination 2	Langbein (1949)	$E_o = 325 + 21T + 0.9T^2$	Budyko (1974)	$AET_{clim2} = P[1 - e^{-\frac{E_o}{P}}]$
Combination 3	Priestley and Taylor (1971)	$E_o = \alpha\frac{\Delta}{\Delta+\gamma}R_n$	Zhang et al. (2001)	$AET_{clim3} = \frac{P[1+w\frac{E_o}{P}]}{1+w\frac{E_o}{P}+(\frac{E_o}{P})}$
Combination 4	FAO Penman–Monteith (Allen, 1998)	$E_o = \frac{0.408\Delta(R_n-G)+\gamma\frac{900}{T_d+273}u_2(e_s-e_a)}{\Delta+\gamma(1+0.34u_2)}$	Zhang et al. (2001)	$AET_{clim4} = \frac{P[1+w\frac{E_o}{P}]}{1+w\frac{E_o}{P}+(\frac{E_o}{P})^{-1}}$

E_o = Potential evapotranspiration, T = Mean annual temperature, P = Total annual precipitation, a = Constant 1.26, A = Slope of the saturation vapor pressure curve, y = Psychrometric constant, R_n = Net radiation calculated by Eq. 40 (Allen, 1998), G = Soil heat flux, T_d = Mean daily temperature, u_2 = wind speed at 2 m above ground surface, e_a = Actual vapor pressure calculated by Eq. 48 (Allen, 1998), e_s = Mean saturation vapor pressure calculated by Eq. 12 (Allen, 1998), w = Plant-available water coefficient (0.5).

was calculated with Eq. (48) of Allen (1998), which is expressed in terms of T_{min}, by assuming that all surfaces are well watered due to the energy limited nature (AET/P < 1) of both the NDB and the MSDB according to Budyko (1974).

Furthermore, the mean elevation used to calculate atmospheric pressure of each CRU cell was obtained from the European Environment Agency's 1 km by 1 km Digital Elevation model (http://www.eea.europa.eu/data-and-maps/data/digital-elevation-model-of-europe). The yearly mean wind data at surface level u_2 required for the FAO Penman–Monteith equation was taken from SMHI's 20th century calculations of geostrospheric wind, specifically for the Triangle 2 of Sweden that covers both the NDB and MSDB (http://www.smhi.se/klimatdata/meteorologi/vind/1.3971). These geostrospheric winds have been shown to correlate well with actual surface wind data (Wern and Bärring, 2009).

The resulting calculated daily E_o per CRU cell was further aggregated to annual values, in order to use the AET_{clim} model of Zhang et al. (2001). The E_o for each basin was finally obtained as the CRU cell area weighted basin average.

3.5. Cultivated area and crop production data

Cultivated area in Sweden has been recorded at county level since the year 1866 by Jordbruksverket (2011). In order to estimate yearly cultivated area in each basin during the period 1901–2002, the percentage of the administrative area of each county falling within each drainage basin was calculated, and then a weighted average was estimated based on the area of each county coinciding with each basin. Due to lack of further information on the historical spatial distribution of cultivated area, this area was assumed to be spread more or less uniformly over each county. Crop production was calculated as the product of cultivated area and crop yield, with the latter being reported since 1913 by Jordbruksverket (2011).

Since cultivated area per county consists of various crop categories recorded throughout the time period, we first calculated production per crop category. When these records included data gaps, missing annual yield values per crop were linearly interpolated between the nearest in time available annual information. Data on yields for certain crops after 1990 were incomplete, so production data after that year does not correspond to total crop production. At any rate, the crops used for the calculations of crop production account for at least 90% of total cultivated area for every year throughout the period 1913–2002, and include winter wheat, winter rye, spring barley, oats, meslin, potatoes, seed grass, green fodder (including the one from cereals and legumes), winter rape, spring rape, winter turnip, spring turnip, fodder roots and linseed.

Seminatural grassland area (from which the cultivated area was mostly developed in the NDB and MSDB) and crop production were obtained from Jordbruksverket (2011), and forest area was obtained from the Forest Statistics of the Swedish National Forest Inventory (http://www.slu.se/en/webbtjanster-miljoanalys/forest-statistics/area/area-tables/). Seminatural grassland and forest areas per drainage basin were calculated similarly as for cultivated area.

4. Results and discussion

During 1901–2002, P increased while R decreased in the NDB (Fig. 2). The reason for this difference in change trends lies to a large degree in the period 1901–1940, when R decreased the most. Throughout the following period 1941–2002, R and P fluctuated more in phase.

The evolution of water storage and its possible change within the NDB can further be estimated from available L data for the main Lake Mälaren in NDB (also shown in Fig. 2), in the absence

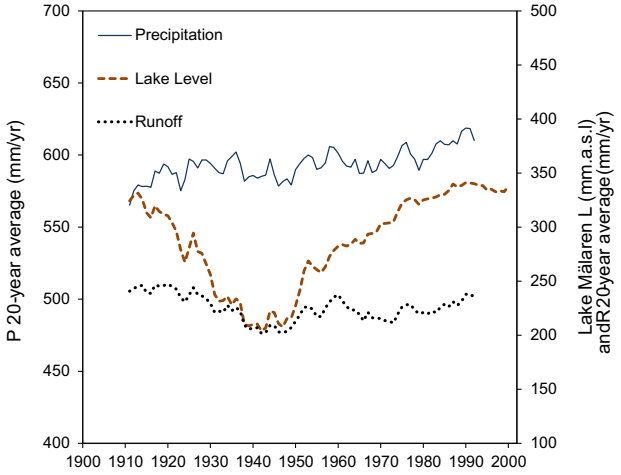

Fig. 2. Hydrological development in the NDB over the 20th century. Total annual precipitation P, total annual runoff R, and mean annual level L, of Lake Mälaren.

of any further level information for the other smaller lakes and the groundwater in the basin. In Lake Mälaren, L decreased steadily during the period 1901–1940 (Fig. 2) reaching its lowest level around 1940 when the lake started to be regulated. As such, it stands to reason that the additional water entering the NDB from the P increase during 1901–1940 left the basin through AET_{wb}, rather than by adding to ΔS within the lake (and basin). Fig. 3 shows then the comparison between AET_{wb} calculated for the three ΔS scenarios presented in Section 3.1. Scenario AET_{wb2} more or less coincides with AET_{wb1}, while AET_{wb3} differs from AET_{wb1} only in the interannual fluctuations and not in its main long term trend. All three methods show increasing AET_{wb} during the period 1901–1940 regardless of the ΔS scenario considered.

The increase seen in all AET_{wb} scenarios from 1901 to 1940 is not explained by the regional hydroclimatic changes during that period as reflected in any of the different AET_{clim} estimates (Table 1), in terms of either their absolute uncalibrated values (Fig. 4a), or their relation to the temporal mean value for each estimate (Fig. 4b). In summary, regardless of ΔS assumption, the hydrological partitioning of P into AET and R shifted to a higher AET level during 1901–1940, from which it did not again decrease during the remaining part of the 20th century (See AET_{wb3}/P line in Fig. 3).

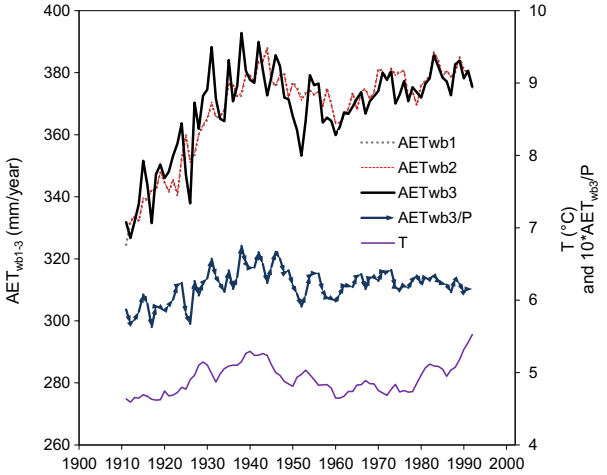

Fig. 3. Temperature and evapotranspiration development in the NDB. The 20-year moving averages for temperature (T), and for data given, water balanced constrained evapotranspiration AET_{wb} for the three different assumption scenarios (AET_{wb1-3}; see Section 3.1) and in relation to precipitation (AET_{wb3}/P).

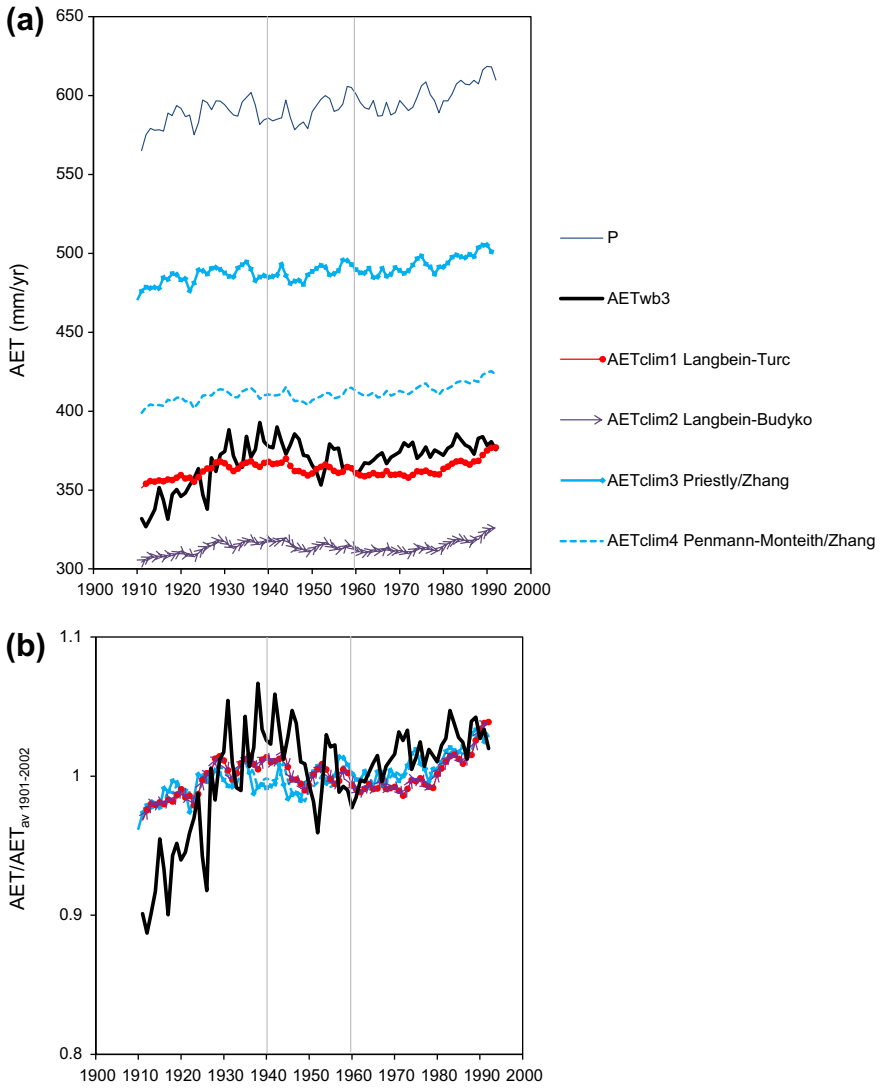

Fig. 4. Development of different estimates of evapotranspiration and precipitation in the NDB. Comparison of the 20-year moving averages of actual evapotranspiration AET_{wb} (exemplified as AET_{wb3} for Scenario 3, Section 3.1) and only climate driven AET_{clim} (based on different methods, see Table 1). (a) Absolute AET values. (b) Relative AET values, normalized by the 1901–2002 mean for each estimation method.

The total increase of AET_{wb3} during 1901–1940 is almost 65 mm/yr (maximum minus minimum limit of the linear AET_{wb3} regression for that period), of which only around 20 mm/yr (31%) is explained by any of the AET_{clim} change estimates. The remaining increase of 45 mm/yr (69%) therefore must have another explanation, which is also further supported by the ANCOVA test of slopes $sAET_{wb3}$ and $sAET_{clim}$, showing that $sAET_{wb}$ is significantly different than any of the different $sAET_{clim}$ results ($\alpha = 0.01$) (Table 2).

Land use changes occurring between 1901 and 1940 can provide the needed explanation for the anomalous AET_{wb} increase (relative to that of all the different AET_{clim} estimates) in that period. The expansion of agriculture was the most important regional landscape change that took place in southern Sweden during the early 20th century. Seminatural grasslands, which were widely used in the 19th century for mowing and grazing, were then converted to cultivated land, mainly grown as ley for fodder and cereal (Cousins, 2001; Jordbruksverket, 2011). During the period 1900–1920, seminatural grasslands accounted for approximately 50% of the cultivated area expansion (Fig. 1b). The remaining cultivated area was gained from conversions of other similar land covers (Jansson et al., 2011).

In the NDB, cultivated area increased continuously during the period 1901–1930 to reach a peak of 470,000 ha or almost 20% of the basin area around 1930 (Fig. 5a). This increase coincides with the first part of the anomalously steep rise in AET_{wb}. The increase in cultivated area was further followed by an increase in crop production, with a first peak occurring shortly before 1940, approximately 10 years after the peak in cultivated area.

The increasing AET_{wb} under the 1901–1940 conditions of cultivated area and crop production in NDB is consistent with: (1) a linear relation between crop biomass production and water vapor flow under similar hydroclimatic conditions (Sinclair et al., 1984), since water availability does not limit growth in this region, and (2) agricultural crops being more productive than the original grassland vegetation. According to data for ley production presented by Jordbruksverket (2011), yields in plowed areas for hay are for instance 2.8 times higher than in unplowed or seminatural grasslands. Note also that, even though crop production could not be estimated before the year 1913, an increasing trend may be expected to have started already from the late 19th century, driven by the increasing cultivated area (Fig. 1b). A small lag of approximately 5 years seen between the AET_{wb} peak and the crop

Table 2
ANCOVA test for difference in the slopes of the linear regressions of the 20-year mean AET_{wb} ($sAET_{wb}$) (exemplified as AET_{wb3} for Scenario 3, Section 3.1) and each AETclim ($sAETclim1–4$) (Section 3.2, Table 1), for each of the periods 1901–1940, 1941–1960, and 1961–2002, for: (a) NDB and (b) MSDB. The slopes in mm/yr^2 of each linear regression are shown in unshaded cells and the probability that the regression lines of AET_{wb} and each AET_{clim} have different slopes is shown in the shaded cells (*P*-value).

		Method 1	Method 2			
		$sAET_{wb3}$	$sAET_{clim1}$	$sAET_{clim2}$	$sAET_{clim3}$	$sAET_{clim4}$
a						
1901–1940	Slope	1.04	0.53	0.46	0.45	0.38
	P-value		*3.17E−09****	*4.99E−10****	*3.98E−09****	*1.38E−10****
1941–1960	Slope	−1.00	−0.22	−0.19	0.47	0.15
	P-value		*0.075*	*0.061*	*2.58E−03****	*0.016*
1961–2002	Slope	0.41	0.51	0.43	0.53	0.44
	P-value		*0.315*	*0.804*	*0.205*	*0.713*
b						
1901–1940	Slope	2.05	0.42	0.36	0.31	0.25
	P-value		*3.89E−09****	*1.20E−09****	*2.97E−09****	*3.41E−10****
1941–1960	Slope	−0.46	*−0.03*	*−0.05*	*0.78*	*0.45*
	P-value		0.314	0.327	6.06E−03***	0.035
1961–2002	Slope	0.87	*0.57*	*0.49*	*0.71*	*0.52*
	P-value		0.177	0,08	0.507	0.122

*** *P*-values show statistically different slopes at the $\alpha = 0.01$ significance level.

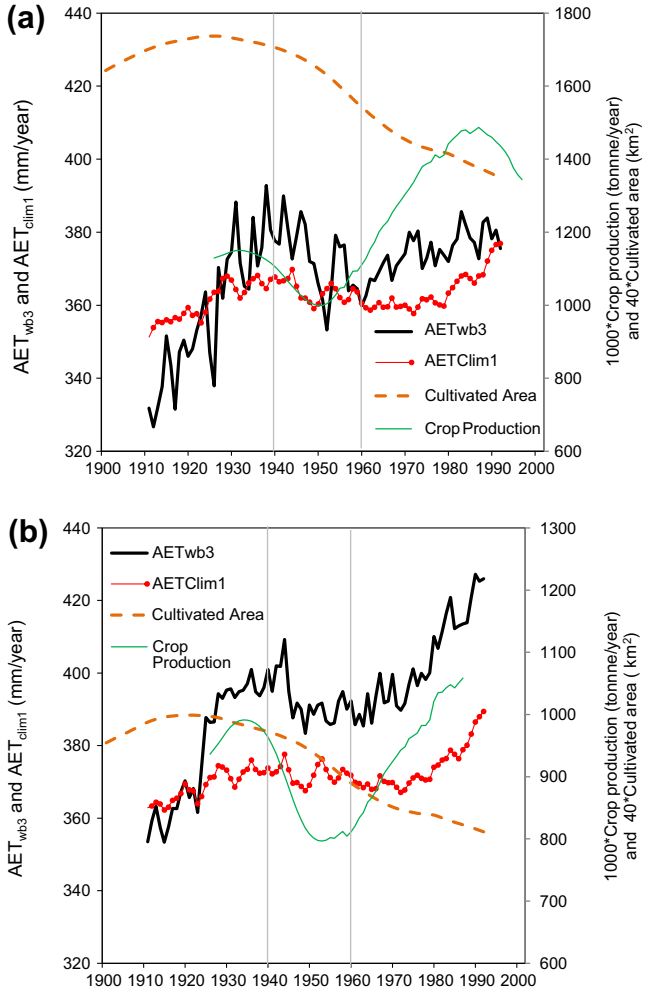

Fig. 5. Evapotranspiration and land use developments in (a) the NDB and (b) the MSDB. Actual evapotranspiration AET_{wb} (exemplified as AET_{wb3} for Scenario 3, Section 3.1) and climate driven estimate example AET_{clim1} (Section 3.2, Table 1), along with cultivated area and crop production during the 20th century.

production peak may further depend on the soil and vegetation continuing to be relatively highly productive (and thereby maintaining relative high rates of evapotranspiration) for some short period after abandonment of a cultivated area, or it may be due to uncertainty in data and/or assumptions underlying the different possible ET_{wb} estimates.

In the period 1940–1960, the cultivated area decreases (Fig. 5a) and the forested area increases (Fig. 1b) while the crop production first decreases somewhat and then increases again to its previous level (Fig. 5a for NDB). In this period, the AET_{clim} estimates and AET_{wb3} mostly decrease (Fig. 4), and $sAET_{wb3}$ differs significantly ($\alpha = 0.01$) from only one $sAET_{clim}$ estimate (AET_{clim3}) (Table 2). Overall, the climate variability and change reflected in the AET_{clim} estimates can to a relatively large degree explain the corresponding variability and change of AET_{wb} in the 1940–1960 period. From 1960 onwards, all AET_{clim} estimates and $sAET_{wb3}$ increase steadily until present times, while $sAET_{wb3}$ is not significantly different from any $sAET_{clim}$ estimate (Table 2). Climate variability and change can thus also in the post-1960 period, with counteracting cultivated area decrease and crop production increase, sufficiently well explain the variability and change in AET_{wb3}.

Overall for the 20th century, we thus find in the NDB an anomalously steep increase of evapotranspiration (relative to that indicated by climate change alone) occurring while cultivated area and crop production were both increasing, or the latter increased while the former remained essentially stable or decreased only mildly. A similar overall codevelopment between AET_{wb} and agricultural expansion is further evident also in the MSDB (Fig. 5b), with $sAET_{wb3}$ being also significantly different ($\alpha = 0.01$) from all $sAET_{clim}$ results in the 1901–1940 period (Table 2b). The NDB and MSDB similarities imply that agricultural development in this period is likely to have shifted AET in the whole region of Southern Sweden, the largest agricultural center of Scandinavia.

Previous studies have mostly linked the development of irrigation to such shifts in evapotranspiration and hydrological flow partitioning in warmer regions, such as Brazil (Loarie et al., 2011), India (Asokan et al., 2010; Douglas et al., 2006), Central Asia (Shibuo et al., 2007) and Australia (Gordon et al., 2003). A recent, comparative study across different regional hydroclimatic and agricultural conditions, however, indicated that development of non-irrigated agriculture may lead to equally large evapotranspiration shifts as irrigation developments (Destouni et al., 2013). The present study has extended the effect analysis for non-irrigated agriculture by considering and testing several different methods for estimating and distinguishing the climate change effects from those of the major land use change, in this case, related with agriculture development.

5. Conclusions

The present multimethod assessment of the hydroclimatic change effects of non-irrigated agriculture have tested and extended the support basis of recent findings (Destouni et al., 2013), indicating considerable evapotranspiration shifts by such agricultural developments. The use of basin wise, water balance constrained and data driven quantification of actual evapotranspiration (AET_{wb}) in direct comparison with multiple different methods of estimating purely climate driven AET_{clim} enabled here a clear distinction between climatic and land use change effects. In the investigated Swedish region, the greatest 20th century shifts of AET in two comparative drainage basins could then be similarly well related to the regional land use conversion from seminatural grasslands to cultivated land and associated enhanced productivity of herbaceous species.

Acknowledgments

This work was funded by the Swedish Research Council (VR; Project Number 2009-3221) and carried out within the framework of the strategic research program EkoKlim at Stockholm University. The authors also thank Else-Marie Wingqvist at the Swedish Meteorology and Hydrological Institute SMHI for the supply of hydrological information and for answers regarding water regulation, Markus Neymad at the Agricultural State Agency Jordbruksverket for his help in understanding the available agricultural information, Per Nilsson and Lars Östlund at the Swedish University of Agricultural Sciences SLU for their advice regarding forest coverage, and Sara Cousins and Regina Lindborg for their help to understand land use changes in the region.

References

Allen, R.G., 1998. Crop Evapotranspiration: Guidelines for Computing Crop Water Requirements, FAO Irrigation and Drainage Paper, 99–0183599-2; 56. FAO, Rome.

Asokan, S.M., Jarsjö, J., Destouni, G., 2010. Vapor flux by evapotranspiration: Effects of changes in climate, land use, and water use. J. Geophys. Res. D: Atmos., 115.

Bonfils, C., Lobell, D., 2007. Empirical evidence for a recent slowdown in irrigation-induced cooling. Proc. Natl. Acad. Sci. USA 104, 13582–13587.

Boucher, O., Myhre, G., Myhre, A., 2004. Direct human influence of irrigation on atmospheric water vapour and climate RID A-3598-2008. Clim. Dyn. 22, 597–603.

Budyko, M.I., 1974. Climate and Life. Academic, New York.

Cheng, L., Xu, Z., Wang, D., Cai, X., 2011. Assessing interannual variability of evapotranspiration at the catchment scale using satellite-based evapotranspiration data sets. Water Resour. Res. 47.

Cousins, S.A.O., 2001. Analysis of land-cover transitions based on 17th and 18th century cadastral maps and aerial photographs. Landscape Ecol. 16, 41–54.

Dahlström, A., Cousins, S.A.O., Eriksson, O., 2006. The history (1620–2003) of land use, people and livestock, and the relationship to present plant species diversity in a rural landscape in Sweden. Environ. History 12, 191–212.

Destouni, G., Darracq, A., 2009. Nutrient cycling and N(2)O emissions in a changing climate: the subsurface water system role. Environ. Res. Lett. 4, 035008 (7pp).

Destouni, G., Asokan, S.M., Jarsjö, J., 2010a. Inland hydro-climatic interaction: effects of human water use on regional climate. Geophys. Res. Lett. 37, L18402.

Destouni, G., Persson, K., Prieto, C., Jarsjö, J., 2010b. General quantification of catchment-scale nutrient and pollutant transport through the subsurface to surface and coastal waters. Environ. Sci. Technol. 44, 2048–2055.

Destouni G., Jaramillo F., Prieto C., 2013. Hydroclimatic shifts driven by human water use for food and energy production. Nat. Clim. Chang., in press. http://dx.doi.org/10.1038/NCLIMATE1719.

Donohue, R.J., Roderick, M.L., McVicar, T.R., 2007. On the importance of including vegetation dynamics in Budyko's hydrological model. Hydrol. Earth Syst. Sci. 11, 983–995.

Douglas, E.M., Niyogi, D., Frolking, S., Yeluripati, J.B., Pielke, R.A., Niyogi, N., Voeroesmarty, C.J., Mohanty, U.C., 2006. Changes in moisture and energy fluxes due to agricultural land use and irrigation in the Indian Monsoon Belt RID A-5015-2009. Geophys. Res. Lett. 33, L14403 (5 pp.).

Gordon, L., Dunlop, M., Foran, B., 2003. Land cover change and water vapour flows: learning from Australia. Philos. Trans.: Biol. Sci. 358, 1973–1984.

Gordon, L., Steffen, W., Jonsson, B., Folke, C., Falkenmark, M., Johannessen, A., 2005. Human modification of global water vapor flows from the land surface RID A-4614-2010 RID C-7651-2011. Proc. Natl. Acad. Sci. USA 102, 7612–7617.

Granström, C., 2003. Vattenståndsmätningar i Mälaren. Väder och Vatten 8.

Jansson, U., Wastenson, L., Aspenberg, P. (Eds.), 2011. Sveriges nationalatlas. Jordbruk och skogsbruk i Sverige sedan år 1900: en kartografisk beskrivning. Norstedt, Stockholm, Sweden.

Jarsjö, J., Asokan, S.M., Prieto, C., Bring, A., Destouni, G., 2012. Hydrological responses to climate change conditioned by historic alterations of land-use and water-use. Hydrol. Earth Syst. Sci. 16, 1335–1347.

Jordbruksverket, 2011. Jordbruket i siffror: åren 1866–2007 = Data tables. [Agriculture in figures years 1866–2007]. Jordbruksverket; Jönköping.

King, M., Kaufman, Y., Menzel, W., Tanre, D., 1992. Remote-sensing of cloud, aerosol, and water-vapor properties from the moderate resolution imaging spectrometer (MODIS) RID C-7153-2011 RID B-8306-2011. IEEE Trans. Geosci. Remote Sensing 30, 2–27.

Karlsson, J., Lyon, S.W., Destouni, G., 2012. Thermokarst lake, hydrological flow and water balance indicators of permafrost change in Western Siberia. J. Hydrol. 464–465, 459–466.

Kueppers, L.M., Snyder, M.A., Sloan, L.C., 2007. Irrigation cooling effect: Regional climate forcing by land-use change RID B-6835-2008. Geophys. Res. Lett. 34, L03703.

Kvalevag, M.M., Myhre, G., Bonan, G., Levis, S., 2010. Anthropogenic land cover changes in a GCM with surface albedo changes based on MODIS data RID A-3598-2008. Int. J. Climatol. 30, 2105–2117.

Langbein, W.B., 1949. Annual runoff in the United States. US Geol. Surv.

Loarie, S.R., Lobell, D.B., Asner, G.P., Mu, Q., Field, C.B., 2011. Direct impacts on local climate of sugar-cane expansion in Brazil RID G-5695-2010. Nat. Clim. Change 1, 105–109.

Lobell, D., Bala, G., Mirin, A., Phillips, T., Maxwell, R., Rotman, D., 2009. Regional differences in the influence of irrigation on climate. J. Clim. 22, 2248–2255.

Mitchell, T., Jones, P., 2005. An improved method of constructing a database of monthly climate observations and associated high-resolution grids RID C-8718-2009. Int. J. Climatol. 25, 693–712.

Norell, B., 2001. Vattenståndsmätningar i Hjälmaren. Väder och Vatten, SMHI, 11.

Priestley, C.H.B., Taylor, R.J., 1971. On the assessment of the surfaceheat flux and evaporation using large-scale parameters. Mon. Weather Rev., 100.

Qiu, G.Y., Yin, J., Tian, F., Geng, S., 2011. Effects of the "conversion of cropland to forest and grassland program" on the water budget of the Jinghe River catchment in China. J. Environ. Qual. 40, 1745–1755.

Saifi, B., Drake, L., 2008. Swedish agriculture during the twentieth century in relation to sustainability. Ecol. Econom. 68, 370–380.

Schilling, K.E., Jha, M.K., Zhang, Y.-K., Gassman, P.W., Wolter, C.F., 2008. Impact of land use and land cover change on the water balance of a large agricultural watershed: historical effects and future directions. Water Resour. Res. 44, W00A09.

Shibuo, Y., Jarsjö, J., Destouni, G., 2007. Hydrological responses to climate change and irrigation in the Aral Sea drainage basin. Geophys. Res. Lett. 34, L21406.

Sinclair, T.R., Tanner, C.B., Bennett, J.M., 1984. Water-use efficiency in crop production. BioScience 34, 36–40.

SMHI, 2010. Swedish Meteorological and Hydrological Institute. Vattenweb. <http://www.vattenweb.smhi.se/>.

Tomer, M.D., Schilling, K.E., 2009. A simple approach to distinguish land-use and climate-change effects on watershed hydrology. J. Hydrol. 376, 24–33.

Turc, L., 1954. The water balance of soils – relation between precipitation evaporation and flow. Ann. Agronomiques, 491–569.

Wang, D., Hejazi, M., 2011. Quantifying the relative contribution of the climate and direct human impacts on mean annual streamflow in the contiguous United States. Water Resour. Res. 47.

Vanlill, W., Kruger, F., Vanwyk, D., 1980. The effect of afforestation with Eucalyptus-grandis hill ex maiden and Pinus-patula schlecht et cham on streamflow from experimental catchments. J. Hydrol. 48, 107–118.

Wern, L., Bärring, L., 2009. Meteorologi Nr 138/2009. Sveriges vindklimat 1901–2008 Analys av förändring i geostrofisk vind.

Zhang, L., Dawes, W.R., Walker, G.R., 2001. Response of mean annual evapotranspiration to vegetation changes at catchment scale. Water Resour. Res. 37, 701–708.

Zhang, K., Kimball, J.S., Nemani, R.R., Running, S.W., 2010. A continuous satellite-derived global record of land surface evapotranspiration from 1983 to 2006 RID B-3227-2012. Water Resour. Res. 46.